HHS Public Access

Author manuscript

Procedia Eng. Author manuscript; available in PMC 2016 August 23.

Published in final edited form as:

Procedia Eng. 2015 ; 124: 213–225. doi:10.1016/j.proeng.2015.10.134.

Highly Symmetric and Congruently Tiled Meshes for Shells and Domes

Muhibur Rasheed[a] and **Chandrajit Bajaj**[a,*]

[a]Computational Visualization Center, Department of Computer Science and Institute of Computational Engineering and Sciences, University of Texas at Austin, Austin, TX 78731, USA

Abstract

We describe the generation of all possible shell and dome shapes that can be uniquely meshed (tiled) using a single type of mesh face (tile), and following a single meshing (tiling) rule that governs the mesh (tile) arrangement with maximal vertex, edge and face symmetries. Such tiling arrangements or congruently tiled meshed shapes, are frequently found in chemical forms (fullerenes or Bucky balls, crystals, quasi-crystals, virus nano shells or capsids), and synthetic shapes (cages, sports domes, modern architectural facades). Congruently tiled meshes are both aesthetic and complete, as they support maximal mesh symmetries with minimal complexity and possess simple generation rules. Here, we generate congruent tilings and meshed shape layouts that satisfy these optimality conditions. Further, the congruent meshes are uniquely mappable to an almost regular 3D polyhedron (or its dual polyhedron) and which exhibits face-transitive (and edge-transitive) congruency with at most two types of vertices (each type transitive to the other). The family of all such congruently meshed polyhedra create a new class of meshed shapes, beyond the well-studied regular, semi-regular and quasi-regular classes, and their duals (platonic, Catalan and Johnson). While our new mesh class is infinite, we prove that there exists a unique mesh parametrization, where each member of the class can be represented by two integer lattice variables, and moreover efficiently constructable.

Keywords

Computational and Combinatorial Geometry; Congruent Tilings; Spherical; Regular; Subdivision; Meshes of Shells; Domes

1. Introduction

Constructions of geodesic domes and spheres have been known since the early 1900s and in fact, several such domes were built even before Goldberg [1] provided a universal design template for constructing an entire family of such domes. This family consists of honeycomb lattices with icosahedral symmetry. Duals of these lattices produce triangulated geodesic domes or spheres. The primary goal of such a design template is to use as few types of tiles/bricks as possible and thereby reduce the dome construction complexity. Very similar design

*Corresponding author: Tel.: +1-512-471-4784; bajaj@cs.utexas.edu.

patterns are also observed at nanoscopic resolution. Viruses, nature's chemical forms, utilize a similar symmetric shell tiling design by pirating its host cell's translational machinery to generate protein tiles from its blueprint (RNA/DNA) (see Figure 1). Even more interestingly, each pair of neighboring proteins (tiles) have the same contact (tile-tile edge) rule, which enables the shell to spontaneously self assemble within the host cell's interior. Such tiled or cage-like structures also suggest applications in the field of nano-materials/nano-fabrication. For example, gold nano-rods have been used in cancer imaging and therapy [2,3], and naturally available virus capsids and protein-cages have been used for targeted drug delivery [4]. Recently, researchers are working on designing protein-cages with specific and custom requirements related to size, tensile strength, deformability, and mass of the cage [5,6].

We propose that such design tasks can be expressed as a geometric optimization problem. Given a target size, one aims to compute the structure of a shell, assembled using several copies of a single building block with a single building rule (how to put two blocks together), such that the overall structure is stable. The issue of stability depends on the material and the physics relevant to the scale of the shell. For nano-cages or virus capsids, one would use chemical interactions and models of molecular energy to assess the strength. On the other hand, for architectural domes, a mechanical analysis of the stress, friction and loading need to be considered. In this paper, we abstract this aspect of stability and only focus on the layout or arrangement of the building blocks. We want to enumerate the family of all possible arrangements which allows symmetric construction using a single type of building block. This is the same as enumerating all possible meshing or tiling of a sphere using a single type of tile (or face) in a symmetric way.

Regular polyhedra are the smallest examples of this type of tiling. They are simultaneously isogonal (vertex-transitive), isotoxal (edge-transitive), and isohedral (face-transitive). In this context, transitivity means that every vertex (or edge or face) are congruent to each other, and for any pair of vertices (or edges or faces), there exists a symmetry preserving transformation of the entire polyhedron which isometrically maps one to the other. Note that two vertices are congruent if they have the same number of edges incident on them with the same angles between the edges; congruency for edges and faces are defined in the general way. There are only 5 regular polyhedra: the tetrahedron, the cube, the octahedron, the dodecahedron and the icosahedron with respectively 4, 6, 8, 12, and 20 faces. Although they seem to have the polyhedral symmetry, more than half of the viruses are formed by more than the number of faces of the corresponding polyhedron. In other words, the building blocks seem to be arranged in a different (denser) layout where the faces of the original polyhedra is subdivided into smaller facets.

Caspar and Klug [7] pioneered the study of such denser symmetric layouts. They showed that the arrangement of building blocks can be modeled using triangular tiles arranged in icosahedral symmetry. A similar class of assembly is seen in fullerene like particles, with 12 pentagonal and many hexagonal faces, which was first characterized by Goldberg [1]. In recent years, several researchers have developed effcient constructions and parameterizations of Goldberg-like particles [8–10]. Deng et al. [11] studied extensions of Goldberg's construction to other platonic solids, but their study is not exhaustive in characterization and enumeration of all the possible cases. In another recent work, Schein and Gayed [12]

developed a numerical optimization scheme that takes a Goldberg-like polyhedra, which may be non-convex and have non-planar faces, and produces strictly convex polyhedra while preserving the edge-lengths. However, the resulting polyhedra no longer have any face-transitivity, and even though the edges have the same length, they are not strictly congruent as their neighboring faces are different-hence making such polyhedra unsuitable for using as layouts for assembly.

In this paper, we provide a formal characterization of the family of meshed polyhedra which are amenable to symmetric assembly. This family contains all polyhedra that are isotoxal and isohedral, but not isogonal. We show that such polyhedra have the global symmetry of one of the Platonic solids, and also introduce *local* symmetries. Furthermore, the family is more general than the Caspar-Klug [7], and Goldberg [1] families, in particular both of those families are subsumed by the new family, dubbed *almost-regular* polyhedra, that we introduce here. In Figure 2, we present a few examples from the family to emphasize the infinite size, the breadth of symmetries, and the existence of polyhedra beyond Caspar-Klug [7], and Goldberg [1] constructions.

In this paper, we additionally show that every member of this family can be generated using a simple technique. The procedure (1) unfolds a Platonic solid onto a 2D lattice of a prescribed symmetry order, (2) embeds the lattice onto the unfolded faces of the solid, and (3) folds it back again, to get a densely tiled polyhedra. We enumerate the possible compatible pairs of platonic solids and 2d lattices, and prove that for each pair, exactly two non-negative integers h and k sufficiently parametrizes the infinite family of *almost-regular* polyhedra that have a global symmetry of the original solid, have congruent faces, congruent edges, and many (uniquely determined by h and k) local symmetries.

This theoretical framework would greatly support design, analysis and construction of symmetric assemblies. For instance, even though combinatorial assembly prediction is an NP-hard problem, using our symmetry characterization, a symmetric assembly of n particles can be predicted using a algorithm whose running time is only polynomial in n [13]. We believe that our results will greatly impact research in several areas including the field of nano-materials, architecture, anti-viral drug discovery etc. For example, understanding of the underlying symmetry and organization have lead to better insights into the stability (e.g. [14,15]), the assembly pathways (e.g. [16–20]), and overall morphology of capsids (e.g. [21,22]), specific biophysical interactions between building blocks (proteins) (e.g. [23–25]), and may also be used as templates for predicting new capsid structures computationally (e.g. [13,26]).

Our work also promises to provide a new technique of regularly meshing arbitrary manifolds. Recent work, especially in the field of computational anatomy [27,28], have explored the possibility of defining a series of diffeomorphic mappings between highly tortous geometries and a simple sphere [29,30], primarily to aid shape comparisons. Hence, we propose that after tiling a sphere using regular tiles using our method, with as much refinement as necessary, one can morph it back onto the manifold to get a regular and quality meshing of the manifold. Such regular meshes are useful for visualization, as well as texture mapping without any crease [31]. This is a valuable alternate to prior techniques which

[32,33] optimize over a 3D rotational symmetric field to generate such meshes. Additionally, our technique guarantees the total number of singularities in the generated mesh (e.g. pentagons in a hexagonal mesh).

In the next section we discuss relevant background and prior work. The following section presents the algorithm for the generation of all possible almost-regular polyhedra, followed by a theoretical analysis of the algorithm which includes (i) a characterization of the family of polyhedra that have face- and edge-transitivity and at most two types of vertices, in terms of local symmetries, (ii) the combinatorics and parametrization of the family, and (iii) the completeness and correctness of the generating algorithm. The next section highlights cases which are topologically correct but has a warped geometry, provides a numerical solution for the curation of such warping, and briefly discusses application of the tiling to predict novel shell structures for virus capsids.

2. Background

The regular polyhedra provide templates for polyhedral symmetry groups. A symmetry group is a set of symmetry operations, each of which maps the corresponding polyhedron to itself, such that the set is closed under composition. The polyhedral symmetry operations can be expressed as pure rotations around different axes through the center of the polyhedra. The points of intersection of these axes with the polyhedra are referred to as the locations of symmetry, and the axes are referred to as the symmetry axes. For instance, the octahedron have 6 axes of 4-fold rotational symmetry[1] going through the four vertices, 8 axes of 3-fold rotational symmetry going through the centers of the faces, and 12 axes of 2-fold rotational symmetry going through the centers of the edges.

2.1. The *Almost-Regular* Polyhedra and Their Duals

We define the family of *almost-regular* polyhedra as all polyhedra which have global polyhedral symmetry, have congruent regular faces, and is face and edge transitive. The first condition means that any such polyhedron must have exactly the same number of rotational symmetry axes with the same symmetry orders as any specific regular polyhedron. We refer to these as the *global* symmetry axes and locations. We shall refer to these global symmetry axes as gv-symmetry axes, ge-symmetry axes and gf-symmetry axes respectively for axes of symmetry going through, respectively, the vertices, edge-centers and face-centers of the regular polyhedron. Additionally, due to the congruency conditions, all vertices, faces and edges of an *almost-regular* polyhedron must have locations of *local* symmetry. Local symmetry operations map the vertices, edges, faces immediately neighboring the location of local symmetry to themselves, but may or may not map the remaining parts of the polyhedron to itself. These axes will be referred to as lv-, le-, and lf-symmetry axes.

While this class bear some similarity with the Catalan solids, an important distinction is that the Catalan solids allow non-symmetric faces (hence, are not isotoxal), as long as all the faces are congruent (for example, the solid in Figure 3(a) is a Catalan solid, but is not almost-regular.

[1] n-fold rotational symmetry, also referred to as the symmetry order n, means that a rotation by $2\pi/n$ maps the polyhedron to itself

Note that, the transitivity properties that make regular polyhedra suitable for assembly, is preserved in almost-regular polyhedra, but now the class is richer and more importantly can model structures with more than 20 building blocks.

The dual of an almost-regular polyhedron has regular faces, is isotoxal and isogonal; but may or may not be isohedral (they can hae at most two types of faces). The closest known family is the semi-regular polyhedra (duals of Catalan solids) which are also isotoxal and isogonal. But the semi-regular polyhedra, which includes the 13 Archimedean solids and the family of prisms with regular faces, have at least 2 types of faces. Figure 4 shows the difference of different classes of polyhedra in terms of their transitivity. Clearly, the *almost-regular* polyhedra have the highest level of symmetry and congruency, after the Platonic solids.

2.2. Related Prior Work

Our construction scheme closely follows the one proposed by Goldberg [1]. The family of polyhedra generated by the Goldberg construction rule [1] are fullerene-like structures. Fullerene-like structures have icosahedral symmetry (symmetry group of the icosahedron), and consists of many hexagonal faces and exactly 12 pentagonal faces. The soccer ball is the smallest example of such structures. See Figure 5 for an illustrative description of the construction.

Caspar and Klug [7] proposed a similar approach, but using a triangular lattice, instead of a hexagonal one, and required that the corners of an edge of the unfolded icosahedron falls on the vertices of the lattice (Figure 5). Since, the triangular lattice is simply the dual of the hexagonal lattice, the mapping is essentially the same. However, the refolded polyhedron now has only regular triangular faces. It has 12 vertices where 5 such faces are incident, and many vertices where 6 faces are incident- the first set are exactly the original vertices of the icosahedron. Notice that this polyhedron is exactly the dual of the one constructed using Goldberg's method.

Polyhedra produced by Caspar and Klug's construction method are a subset of the *almost-regular* family, and the ones produced by Goldberg's are their duals. In a related work, Pawley [34] studied other ways of wrapping different polyhedra using different lattices from the wallpaper group and identified more tiled polyhedra which would fall in the *almost-regular* family. However, Pawley did not provide any theoretical characterization of the factors related to the possibility or impossibility of such wrappings, or the completeness of the construction. We address this issue in our construction.

3. Construction and Combinatorics of Families of *Almost-regular* Polyhedra

3.1. TilingGen: an algorithm for generating all *almost-regular* polyhedra

We present a simple algorithm for generating all *almost-regular* polyhedra (see Figure 6).

3.2. Characterizing All Possible *Almost-Regular* Polyhedra and Completeness of TilingGen

Both Goldberg and Caspar-Klug constructions can be expressed as unfolding a regular polyhedron onto a 2D lattice and then refolding it with the lattice etched onto its faces.

Pawley's wrapping idea is equivalent. We call this the *unfold-etch-refold* method. Here, we prove the conditions that must be satisfied to produce almost-regular polyhedra using the *unfold-etch-refold* mrthod for any regular solid, unfolded in any way, onto any 2D lattice.

Shepherd's conjecture [35] states that all convex polyhedra have a non self-overlapping planar unfolding with only edge-cuts. This conjecture is not proved or disproved yet for all possible convex polyhedra. However, for the set of special classes we are interested in, it is true. Hence, in principle it is possible to unfold one such polyhedra and lay it down on a 2D grid, use the grid to draw tiles of the unfolded polyhedron, and then fold it back up to get a tiled polyhdron. However, every polyhedron actually has many unfoldings. For example, icosahedron have 43380 unique unfoldings. Caspar and Klug's construction produced almost-regular polyhedra using 1 such unfolding, but it is not clear whether other unfoldings would also produce similar *almost-regular* polyhedra, or different types of *almost-regular* polyhedra, or not be *almost-regular*. To address this question, we have characterized [36] the relationship of the local and global symmetries of the almost-regular polyhedra, and the etched polyhedra (henceforth called *tiling*) produced using unfold-etch-refold construction. Here we only report the theoretical conclusion

Theorem 3.1: *The polyhedron generated by an* unfold-etch-refold *is* almost-regular *if and only if a compatible mapping of a regular polyhedron onto an* unfold-etch-refold *compatible lattice is performed.*

Please see [36] for detailed enumeration of possible compatible mapping of a regular polyhedron onto an *unfold-etch-refold* compatible lattice, and proof of the above theorem and associated lemmas.

Figure 7 shows a few examples of constructing *almost-regular* polyhedron and their duals by compatible mapping of a face of a regular polyhedron on a *unfold-etch-refold* compatible lattice. Note that the etched-faces that cross an edge of $\mathscr{T}$ are geometrically not identical to the ones that do not. The ones crossing the boundary have a crease inside them, or if they are flattened, they are no longer regular. This is addressed in the Section 4.1.

3.3. Parametrization and Geometric Aspects of TilingGen

The theoretical characterization of compatible mappings in the *unfold-etch-refold* protocol immediately lends itself to a simple parametrization of the *almost-regular* family. Furthermore, the symmetry at global and local levels lets us represent the geometry using a minimal set of points. Both of these insights are used in TilingGen.

For the sake of simplicity of presentation, the discussion in this section, in most cases, is focused solely on mapping icosahedron onto triangular lattices. Other compatible mappings can be discussed in the same manner with almost no difference in the theorems/lemmas presented here except for minor changes in counting. The choice to focus on the icosahedral case is primarily due to two reasons- first, it has the highest level of symmetry among the regular polyhedra which have a compatible mapping, and second, it has applications in modeling viruses, fullerenes etc.

3.3.1. Parametrization—Let $\mathcal{L}$ be a lattice with origin O and axes H and K. Any point in the lattice is expressed using coordinates (h,k) where both h and k are integers. Below we mention results (whose proofs can be found in [36]) which establish that a simple tuple $<\mathcal{P},\mathcal{L},h,k>$ is sufficient to represent the topology of a specific *almost-regular* polyhedron.

Lemma 3.2: *Assuming that one corner A of the face $\mathcal{T}$ of the polyhedron is mapped to the origin O of the lattice (or the nearest face-center for dual constructions). Then specifying the position of another compatibly placed point B(h,k) is sufficient to parametrize the entire mapping.*

Lemma 3.3: *Topology of any* almost-regular *polyhedron or its dual can be expressed using a tuple $<\mathcal{P},\mathcal{L},h,k>$, where $\mathcal{P}$ is a regular polyhedron, $\mathcal{L}$ is a lattice represented using two axes, and h and k are integers.*

3.3.2. Combinatorics and Symmetry—We consider the case where $\mathcal{P}$ is the icosahedron whose symmetry group will be denoted as I, and $\mathcal{L}$ is the triangular lattice which will be denoted as $\mathcal{L}^3$. Now, we discuss some properties of the lattice.

Definition 3.4: *We define each triangle of the lattice $\mathcal{L}^3$ as a small triangle and use t to denote such a triangle. Let us define a triple $<i,j,k>$ where i and j are integers and $k \in \{+,-\}$. Let the triangle produced by the intersections of the lines $h = i$, $k = j$ and $h + k = i + j + 1$ (having the vertices $(i,j),(i+1,j)$ and $(i,j+1)$) be denoted t_{ij+}. Similarly, the triangle denoted t_{ij-} has vertices $(i,j),(i+1,j-1)$ and $(i+1,j)$, and is produced by the intersections of the lines $h = i+1$, $k = j$ and $h + k = i + j$.*

The proof of the following lemma is immediate from this definition.

Lemma 3.5: *$t_{i_1j_1k_1}$ coincide with $t_{i_2j_2k_2}$ if and only if $i_1 = i_2$, $j_1 = j_2$ and $k_1 = k_2$. For any small triangle in $\mathcal{L}^3$, there exists a triple $<i,j,k>$ such that t_{ijk} represents that small triangle.*

Through etching, the triangular lattice $\mathcal{L}^3$ produces a tiling of a face $\mathcal{T}$ (which will be called a large triangle in this section) of $\mathcal{P}$ where each tile is a small triangle. Now we consider some properties of this tiling.

Assuming A is at (0,0), B is (h,k) such that h and k are integers, the tiling produced by $\mathcal{L}^3$ on $\mathcal{T}$ satisfies:

- The area of $\mathcal{T}$ is $\frac{\sqrt{3}}{4}(h^2+hk+k^2)$, which is equal to the area of h^2+hk+k^2 small triangles.
- In addition to A,B and C, $\mathcal{T}$ includes exactly $\frac{h^2+hk+k^2-1}{2}$ more vertices of $\mathcal{L}^3$. Note that any vertex that lie on an edge of $\mathcal{T}$ is counted as half a vertex.
- Each edge of $\mathcal{T}$ is intersected by at most $2(h+k)-3$ lines of the form $h = c$, $k = d$ and $h + k = e$, where c,d and e are integers.

The number of small triangles intersected by any edge of $\mathscr{T}$ is at most $2(h+k-1)$.

The following are some combinatorial properties of the overall tiled polyhedron-

- There are exactly $20(h^2+hk+k^2)$ small triangles, and the same number of local 3-fold axes.
- The 12 gf-symmetry axes are surrounded by 5 small triangles.
- There are exactly $10(h^2+hk+k^2-1)$ vertices (not lying on the gf-axes) with 6-fold local symmetry.

Similar properties can easily be derived for other mappings as well. The important point to note is that not only the topology, but also the symmetry and combinatorics are also parameterized by only h and k.

3.3.3. Topology to Geometry—Note that given a point P with coordinate (i, j) inside $\mathscr{T}$, there exists two other points Q and R such that P, Q and R are 3-fold symmetric around the center D of $\mathscr{T}$. The two points Q and R have coordinates $(h-i-j,k+i)$ and $(h+k+j,-h-i)$ respectively. This can be seen by noticing that stepping along the H and K axis by i and j units from $A(0,0)$ is C^3 symmetric (around D) to stepping in $-H+K$ and $-H$ directions by the same units from $B(h,k)$, and stepping in $-K$ and $H-K$ directions by the same units from C. We can further extend it to triangles and deduce the following.

Lemma 3.6: *If* $A(h_1,k_1)$, $B(h_2,k_2)$ *and* $C(h_3,k_3)$ *are three points in the HK coordinate system such that* h_1,h_2,h_3,k_1,k_2,k_3 *are integers and ABC is an equilateral triangle whose centroid is O, then the small triangles* $t_{h_1+i,k_1+j,\pm}$, $t_{h_2-i-j-1,k_2+i,\pm}$ *and* $t_{h_3+j,k_3-i-j-1,\pm}$ *are* C^3 *symmetric around O.*

Now, we define the minimal set of points or non-redundant set of points $\mathbb{S}$ such that no two points $s_i, s_j \in S$ are C^3 symmetric to each other around D, and all points in $\mathbb{S}$ lie inside or on $\mathscr{T}$. Clearly, $|\mathbb{S}| = \lceil \frac{h^2+hk+k^2}{3} \rceil$. Note that applying C^3 operations on $\mathbb{S}$ produces all points inside and on $\mathscr{T}$.

We conclude with the following theorem, whose proof is in [36]

Theorem 3.7: *The algorithm* TilingGen *constructs a minimal geometric representation of the* almost-regular *polyhedron in terms a set of points* $\mathbb{S}$ *embedded onto the XY plane and a set of 3D transformations* $\mathbb{T}_{all}$.

4. Results

Some polyhedra generated by applying TilingGen are shown in Figure 8.

Note that the tiles that cross the boundaries of a face $\mathscr{T}$ of $\mathscr{P}$ may have a crease along the edge of the $\mathscr{T}$. This is a result of the *unfold-etch-refold* technique. Tiles generated by this algorithm will also have the same problem and such tiles will be non-regular, and in some cases even non-planar.

4.1. Curation of Tiles

As mentioned before, sometimes the lattice faces, which corresponds to tiles/faces of the generated *almost-regular* polyhderon, crosses the boundary of the polyhedral face $\mathscr{T}$ embedded on the lattice. During folding, these faces get warped. There can be exactly three types of scenarios (for mapping to a square or triangular lattice).

1. If one corner of $\mathscr{T}$ is at (0,0), and the other corner is at (h,k) such that either $h = 0$ or $k = 0$, then no lattice face crosses the edges of $\mathscr{T}$, and no curation is required. (see Figure 9 top row).
2. If one corner of $\mathscr{T}$ is at (0,0), and the other corner is at (h,k) such that $h = k$ then some lattice faces are exactly bisected by the edges of $\mathscr{T}$. The curation is quite trivial in this case. If $h = k$, the center of $\mathscr{T}$ would lie on a lattice vertex. Let the center be D, and the face $\mathscr{T}$ be ABC. Then, folding along AD, BD and CD will not warp any lattice face. Additionally, connecting D to the centers of the neighboring polyhedral faces $\mathscr{T}$ would satisfy all global symmetry conditions as well. This folding will produce a base polytope which actually looks like the *almost-regular* polyhedron with $h = k = 1$. In fact, for any integer i, to polyhedron generated for $h = k = i$ is nothing but subdivisions of the faces of the $h = k = 1$ polyhedron. Interestingly, in some cases, the new folding produces a polyhedron with base geometry like some Catalan solids, but will unlike Catalan solids, these will have regular faces and may be non-convex. For example, the $h = k = 1$ polyhedron have the same topology as the pentakis dodecahedron (see Figure 9 middle row).
3. If one corner of $\mathscr{T}$ is at (0,0), and the other corner is at (h,k) such that $h = k, \& h, k > 0$; then, for all mappings on the hexagonal lattice, some lattice faces shall cross the edges of $\mathscr{T}$ in variable ways. There does not exist any folding which can avoid the crossing while maintaining global symmetry (as the lines will not meet at the center of the face $\mathscr{T}$). See Figure 9 bottom row. In this case, no exact solution exists, and we provide a numerical approximation which maximizes the regularity while ensuring that global symmetries are not violated (see below).

We should mention that recently Mannige and Brooks [37] explored such pseudo-irregularities in icosahedral tilings and suggested the existence of three classes depending on the values of h and k. Here, we have generalized that to all *almost-regular* polyhedra, and quantified the exact number of faces that gets warped.

4.1.1. Curation as a Numerical Optimization Problem—The goal of curation would be to make all the faces as regular as possible without violating global symmetry. A similar problem specifically for the family of polyhedra generated by mapping an icosahedron onto a hexagonal lattice was addressed in [12]. In that work Schein and Gayed aimed to make all the hexagonal faces that cross the face boundary, and become creased/non-planar, into planar ones while keeping the edge lengths equal. They also showed that it is possible to provide an effcient numerical solution to the problem which ensures that no two hexagonal/pentagonal

tiles lie on the same plane and the overall polyhedron is convex. However, the shapes of the hexagons are allowed to get distorted such that the angles are no longer equal, and may vary a lot within the same hexagon. Hence, the faces are no longer congruent (or even nearly congruent) to each other. This makes such a polyhedron non-amenable for modeling structures formed using a single type of building block, for instance viral capsids. In contrast, we want to maintain the congruence of the tiles as much as possible.

When mapping a polyhedron onto a triangular lattice, the generated polyhedra falls under the class called Deltahedra, polyhedra whose faces are all equilateral triangles. Even though there are an infinite family of Deltahedra [38] (our families are also infinite), it has been known since Freudenthal and van der Waerden's work [39], that there are exactly eight convex Deltahedra, having 4, 6, 8, 10, 12, 14, 16 and 20 faces; among them only three are regular or have symmetries like the regular ones. So, our family of *almost-regular* polyhedra cannot be convex and regular at the same time. We have prioritized regularity in our scheme.

- Let the set of all points on the generated polyhedron be $\mathbb{S}_{all} = \mathbb{T}_{all}(\mathbb{S}$.
- Let $\mathbb{E}_1$ be the set of lattice/tile edges on the generated polyhedron
- Let $\mathbb{E}_2$ be the set of diagonals of all the tiles on the generated polyhedron
- Let, for any point $p \in \mathbb{S}_{all}$, the functions $s(p)$ and $t(p)$ returns respectively a point $q \in \mathbb{S}$and a transformation $T \in \mathbb{T}_{all}$ such that $p = T(q)$.
- Let $dist(u,v)$ is the square of the Euclidean distance between two points.

In our calculations we shall only update the positions of the points in $\mathbb{S}$ and all other points $p \in \mathbb{S}_{all}$ on the polyhedron will be generated as $t(u)(s(u))$. This ensures that the points are always moved in a symmetric way with respect to the global symmetry axes. Hence global symmetry is never violated.

Let $\mathbb{S}^0$ be the initial positions of the points in $\mathbb{S}$ As we update the locations of the points in $\mathbb{S}$ in our algorithm, the squared displacement of each point $p \in \mathbb{S}$will be defined as $\delta(p) = (dist(p,p^0))^2$, where $p^0 \in \mathbb{S}^0$ is the initial position of p. Also, the squared length of a line segment $e(u,v) \in \mathbb{E}_1 \cap \mathbb{E}_2$ will be computed as $dist(t(u)(s(u)),t(v)(s(v)))^2$ and be denoted $l(e)$.

Let us also define $\mu_1 = \frac{1}{|\mathbb{E}_1|}\sum_{e\in\mathbb{E}_1}(l(e))$ and $\mu_2 = \frac{1}{|\mathbb{E}_2|}\sum_{e\in\mathbb{E}_2}(l(e))$

Finally, we define an energy function $\mathbb{F}\mathbb{S}$ as follows:

$$\mathcal{F}(\mathbb{S}) = \frac{1}{|\mathbb{E}_1|}\left(\sum_{e\in\mathbb{E}_1}(l(e)-\mu_1)\right) + \frac{1}{|\mathbb{E}_2|}\left(\sum_{e\in\mathbb{E}_2}(l(e)-\mu_2)\right) + \frac{1}{|\ |}\left(\sum_{p\in\mathbb{S}}\delta(p)\right).$$

Now, we minimize the function $\mathbb{F}\mathbb{S}$ over the positions of the points in $\mathbb{S}$

This is clearly a quadratic optimization problem over $h^2 + hk + k^2$ variables, and for most practical values of h and k it can be solved efficiently using any numerical solution techniques. We chose to use the limited memory variant of Broyden Fletcher Goldfarb Shanno (BFGS) algorithm [40] due to its faster convergence rates. Also since first and second derivatives (hessian) of the energy function are straight-forward to compute, the

numerical solution does not require finite-differences and heuristic based hessians, making the solution under BFGS more efficient and stable. Figure 10 shows some examples of numerically curating warped faces.

4.2. Application of Meshed Polyhedra to Construct Shell Structures

Viruses, as discussed before, have icosahedral symmetric shells formed by multiple copies of the same protein. While several existing works (e.g. [16–20,23–25]) leverage symmetry to analyze a given shell structure, we are the first to propose a generative algorithm to predict all such structures.

We propose that each virus shell is templated on a particular *almost-regular* polyhedron. We consider the assmebly prediction problem where the number of proteins and the structure of a individual protein is known, and the structure of the whole shell is unknown and must be predicted. We propose the following generation algorithm (Figure 11) to solve this problem. Note that, while the algorithm specifies icosahedral symmetry as that is the relevant one for viruses, it can easily be extended to handle other cases.

Please see our arxiv technical report [36] for details of the decoration procedure (the symmetric placement and transformation of super-blocks onto tiles).

4.2.1. Reproducing Known Shell Structures—To verify the effectiveness of the tiling and decoration algorithms, we applied it to predict shell structures for some viruses for which the sturcture of the individual building blocks (proteins), as well as the entire shell is known. We show some examples here.

In Figure 13(a), we present the results of modeling the Tobacco Necrosis Virus which has 60 proteins on its shell. We templated it based on a polyhedra with h=1, k=0 and the resulting computationally predicted shell had less that 5A RMSD error with respect to the known shell. This error is considered acceptable in molecular biology community. There is no topological errors. We had similar success in predicting the structure of Nudaurelia Capensis Virus which requires 240 proteins on its shell and the template polyhedra was constructed with h=2, k=0 (Figure 13(b)). Finally, Figure 13(c–d) show the outcome of predicting the shell of Rice Dwarf Virus which has 780 proteins. The layout for this can be either a polyhedra with h=3, k=1; or h=1, k=3; the latter is topologically incorrect if compared to the shell found in nature. Unfortunately, our geometric optimization algorithm and scoring model cannot discriminate between the two.

4.2.2. Assembling Multiple Sized Shells Using the Same Building Block—In Figure 12 we show that our algorithm can easily produce shells of different sizes using the same building blocks. Here we used the same protein, but decorated tilings of different complexities and reported the highest scoring models for each size.

5. Conclusion

Our congruent meshing technique provably generates all possible shell and dome shapes. These shapes can be uniquely meshed (tiled) using a single type of tile (mesh face), and

follows a single tiling (meshing) rule that governs the mesh arrangement with maximal vertex, edge and face symmetries. Additionally, when considering the geometric aspects of the congruently tiled meshes, we characterized the cases where the faces may become non-regular, and provided meshing solutions for each case. Moreover, we point out that our class of a congruent faced polyhedron is not similar to prior known families like Catalan solids, Johnson solids, or Archimedean solids. Our mesh construction rules generate a new and rich family with high levels of symmetry. Some Catalan solids like the Tetrakis Hexahedron, Triakis Octahedron, Triakis Icosahedron, Rhombic Dodecahedron, Rhombic Triacontahedron, or Pentakis Dodecahedron may seem like they satisfy the properties of *almost-regular* polyhedron, but actually all of them violate either the global or the local symmetry conditions. Also Archimedean solids like the truncated cube can be generated by placing the triangular faces of a tetrahedron on a hexagonal lattice, such that the corners of each triangle fall on the centers of 3 surrounding hexagonal faces. Many other Archimedian solids are isogonal and isotoxal, but none of them (not even the truncated cube) are duals of of any *almost-regular* polyhedron. Our characterization and tiling construction algorithm additionally provide automatic templates in computational design and analysis of dome or spherical shaped objects with symmetry and regular tiles. There are additional applications in designing nano-cages for drug delivery and cancer therapy, designing easy to assemble masonry structures etc. Additionally, the regular and congruent tilings we produce promises to be an interesting template for arbitrarily refined meshing of manifolds, using diffeomorphic mappings between the manifold and a sphere.

Acknowledgments

This research was supported in part by NSF:OCI-1216701 and Sandia Natl. Lab-1439100.

References

1. Goldberg M. A class of multi-symmetric polyhedra. Tohoku Mathematical Journal. 1937:104–108.
2. Chen J, Saeki F, Wiley BJ, Cang H, Cobb MJ, Li ZY, Au L, Zhang H, Kimmey MB, Li X, et al. Gold nanocages: Bioconjugation and their potential use as optical imaging contrast agents. Nano Letters. 2005; 5:473–477. [PubMed: 15755097]
3. Xia X, Xia Y. Gold nanocages as multifunctional materials for nanomedicine. Frontiers of Physics. 2014; 9:378–384.
4. Shi J, Votruba AR, Farokhzad OC, Langer R. Nanotechnology in drug delivery and tissue engineering: From discovery to applications. Nano Letters. 2010; 10:3223–3230. [PubMed: 20726522]
5. Steinmetz NF, Lin T, Lomonossoff GP, Johnson JE. Structure-based engineering of an icosahedral virus for nanomedicine and nanotechnology. Current Topics in Microbiology and Immunology. 2009; 327:23–58. [PubMed: 19198569]
6. Shang W, Liu J, Yang J, Hu Z, Rao X. Dengue virus-like particles: Construction and application. Applied Microbiology and Biotechnology. 2012; 94:39–46. [PubMed: 22382168]
7. Caspar, DL.; Klug, A. Physical principles in the construction of regular viruses. Cold Spring Harbor Symposium on Quantitative Biology; 1962. p. 1-24.
8. Hu G, Qiu WY. Extended goldberg polyhedra. Communications in Mathematical and in Computer Chemistry. 2008; 59:585–594.
9. Schwerdtfeger P, Wirz L, Avery J. Program fullerene: A software package for constructing and analyzing structures of regular fullerenes. Journal of Computational Chemistry. 2013; 34:1508–1526. [PubMed: 23559399]

10. Fowler PW, Rogers KM. Spiral codes and goldberg representations of icosahedral fullerenes and octahedral analogues. Journal of Chemical Information and Computer Sciences. 2001; 41:108–111. [PubMed: 11206362]
11. Deng T, Yu ML, Hu G, Qiu WY. The architecture and growth of extended platonic polyhedra. Communications in Mathematical and in Computer Chemistry. 2012; 67:713–730.
12. Schein S, Gayed JM. Fourth class of convex equilateral polyhedron with polyhedral symmetry related to fullerenes and viruses. Proceedings of the National Academy of Sciences of the United States of America. 2014; 111:2920–5. [PubMed: 24516137]
13. Rasheed, M.; Bajaj, C. Technical Report 14–24. Institute of Computational Engineering and Sciences, The University of Texas at Austin; Austin, Texas, USA: 2014. Predicting symmetric spherical shell assemblies.
14. Mateu MG. Assembly, stability and dynamics of virus capsids. Archives of Biochemistry and Biophysics. 2012
15. Peeters K, Taormina A. Group theory of icosahedral virus capsid vibrations: a top-down approach. Journal of Theoretical Biology. 2009; 256:607–624. [PubMed: 19014954]
16. Berger B, Shor PW, Tucker-Kellogg L, King J. Local rule-based theory of virus shell assembly. Proceedings of the National Academy of Sciences of the United States of America. 1994; 91:7732–7736. [PubMed: 8052652]
17. Zlotnick A. Theoretical aspects of virus capsid assembly. Journal of Molecular Recognition. 2005; 18:479–490. [PubMed: 16193532]
18. Zandi R, Reguera D, Bruinsma RF, Gelbart WM, Rudnick J. Origin of icosahedral symmetry in viruses. Proceedings of the National Academy of Sciences of the United States of America. 2004; 101:15556–15560. [PubMed: 15486087]
19. Rapaport D. Self-assembly of polyhedral shells: A molecular dynamics study. Physical Review E. 2004; 70:1–13.
20. Bona M, Sitharam M, Vince A. Enumeration of viral capsid assembly pathways: tree orbits under permutation group action. Bulletin of Mathematical Biology. 2011; 73:726–753. [PubMed: 21174231]
21. Mannige RV, Brooks CL III. Tilable nature of virus capsids and the role of topological constraints in natural capsid design. Physical Review E (Statistical, Nonlinear, and Soft Matter Physics). 2008; 77:051902–9.
22. May ER, Brooks CL. On the morphology of viral capsids: Elastic properties and buckling transitions. The Journal of Physical Chemistry B. 2012; 116:8604–9. [PubMed: 22409201]
23. Bahadur RP, Rodier F, Janin J. A dissection of the protein-protein interfaces in icosahedral virus capsids. Journal of Molecular Biology. 2007; 367:574–590. [PubMed: 17270209]
24. Carrillo-Tripp M, Brooks CL, Reddy VS. A novel method to map and compare protein-protein interactions in spherical viral capsids. Proteins. 2008; 73:644–655. [PubMed: 18491385]
25. Cheng S, Brooks CL. Viral capsid proteins are segregated in structural fold space. PLoS Computational Biology. 2013; 9:e1002905. [PubMed: 23408879]
26. Andre I, Bradley P, Wang C, Baker D. Prediction of the structure of symmetrical protein assemblies. PNAS. 2007; 104:17656–17661. [PubMed: 17978193]
27. Grenander U, Miller MI. Computational anatomy: An emerging discipline. Quarterly of Applied Mathematics. 1998; 56:617–694.
28. Miller MI, Priebe CE, Qiu A, Fischl B, Kolasny A, Brown T, Park Y, Ratnanather JT, Busa E, Jovicich J, et al. Collaborative computational anatomy: an mri morphometry study of the human brain via diffeomorphic metric mapping. Human Brain Mapping. 2009; 30:2132–2141. [PubMed: 18781592]
29. Beg MF, Miller MI, Trouvé A, Younes L. Computing large deformation metric mappings via geodesic flows of diffeomorphisms. International Journal of Computer Vision. 2005; 61:139–157.
30. Glaunès J, Qiu A, Miller MI, Younes L. Large deformation diffeomorphic metric curve mapping. International Journal of Computer Vision. 2008; 80:317–336. [PubMed: 20419045]
31. Liu, Y.; Lin, W-C.; Hays, J. ACM Transactions on Graphics (TOG). Vol. 23. ACM; 2004. Near-regular texture analysis and manipulation; p. 368-376.

32. Dong S, Kircher S, Garland M. Harmonic functions for quadrilateral remeshing of arbitrary manifolds. Computer Aided Geometric Design. 2005; 22:392–423.
33. Nieser M, Palacios J, Polthier K, Zhang E. Hexagonal global parameterization of arbitrary surfaces, Visualization and Computer Graphics. IEEE Transactions on. 2012; 18:865–878.
34. Pawley G. Plane groups on polyhedra. Acta Crystallographica. 1961; 15:49–53.
35. Shephard GC. Convex polytopes with convex nets. Mathetical Processdings of the Cambridge Philosophical Society. 1975; 78:389–403.
36. Rasheed, M.; Bajaj, C. Characterization and construction of a family of highly symmetric spherical polyhedra with application in modeling self-assembling structures. 2015. http://arxiv.org/abs/1507.08374
37. Mannige RV, Brooks CL. Periodic table of virus capsids: Implications for natural selection and design. PLoS ONE. 2010; 5:7.
38. Trigg CW. An infinite class of deltahedra. Mathematics Magazine. 1978; 51:5557.
39. Freudenthal H, van der Waerden BL. Over een bewering van euclides (on an assertion of euclid). Simon Stevin (in Dutch). 1947; 25:115128.
40. Byrd RH, Lu P, Nocedal J, Zhu C. A limited memory algorithm for bound constrained optimization. SIAM Journal on Scientific Computing. 1995; 16:1190–1208.

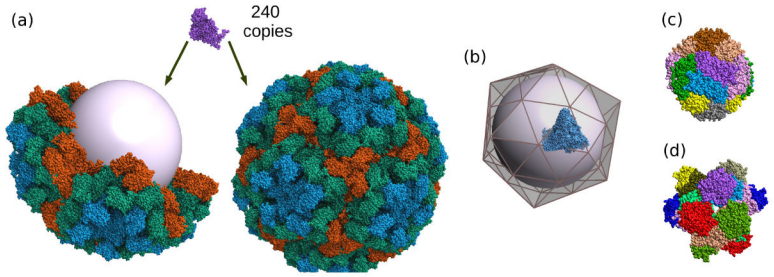

Fig. 1. Motivation for studying congruent meshed polyhedra

(a) Most viruses have a symmetric shell protecting its genome (shown only as a sphere in the figure). The shell is formed by multiple copies of a single building block (protein) arranged symmetrically. (b) The arrangement of the proteins for the virus shown in (a) uniquely maps to a tiled polyhedra with icosahedral symmetry. The polyhedra sufficiently characterizes all relevant symmetry and topology information and serves as a template for the analysis, prediction and construction of such shells. (c–d) Shell structures in nature also comes in octahedral and tetrahedral symmetries. Our class of polyhedra covers all these cases.

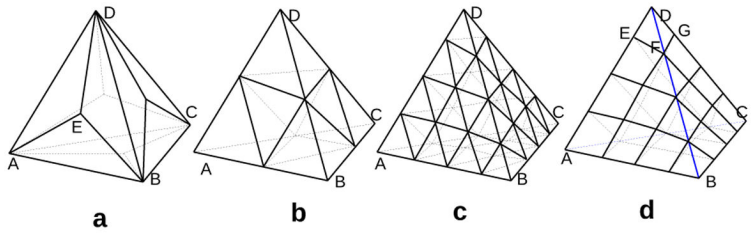

Fig. 2. A small sample from our family of *almost-regular* polyhedra

The family provides infinite series of polyhedra having the same global and local symmetries, using the same type of tiles and inter-tile matching rule (or edges). For example, (a–c) shows three examples having octahedral symmetries but using 1352, 392 and 504 tiles respectively. This allows the design of progressively finer meshes, or enables templating for larger structures using the same building block. The family also covers multiple types of global symmetries. For example, in (d), we see a mesh with icosahedral symmetry but using almost the same number of tiles as (a). Finally, our construction also supports other regular tilings, for example hexagonal honeycomb tilings shown in (e–f) with tetrahedral and octahedral global symmetries respectively. Note that the examples shown in (a–c) and (e–f) do not fall under the classic Goldberg construction.

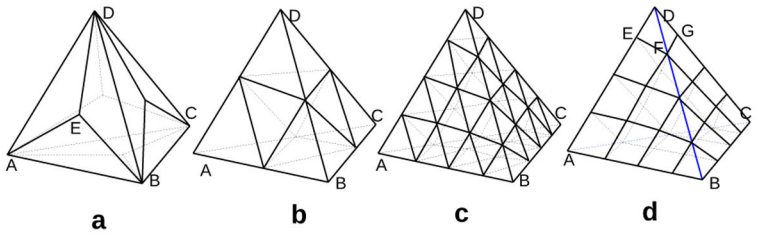

Fig. 3. Illustration of the criterion for almost-regular polyhedra

The polyhedra shown in **(a)** and **(d)** are not almost-regular. In **(a)**, the global symmetries are preserved, but the local symmetries are not (for example, it is not locally 2-fold symmetric around the center of DE). In **(d)**, local symmetries are intact, but the global 3-fold symmetries are not (for example, around the center of ABD).

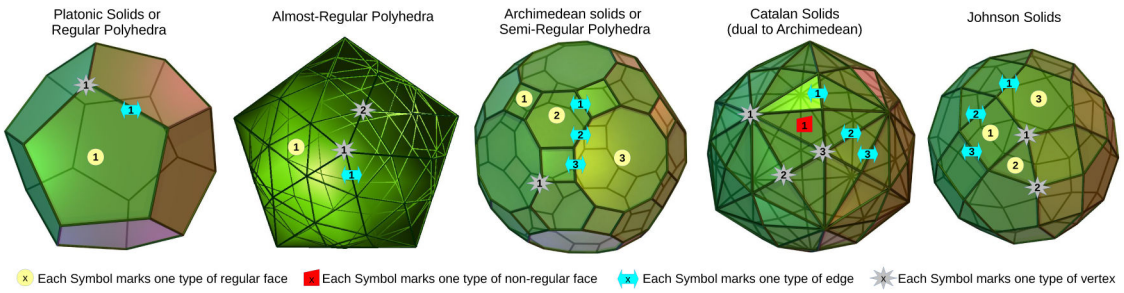

	Regular	Almost-regular	Dual of Almost-regular	Semi-regular	Dual of Semi-regular	Johnson solid
Every face is regular	Y	Y	Y	Y	N	Y
Every face is congruent	Y	Y	At most 2 types	At least 2 types	Y	N
Every edge is congruent (has the same polygonal face on its sides)	Y	Y	Y	N	N	N
Every vertex is congruent (has the same number and type of faces incident on it)	Y	At most 2 types	Y	Y	At least 2 types	N

Fig. 4. Illustration of different classes of symmetric polyhedra

We show example polyhedra from regular, *almost-regular*, semi-regular, duals of semi-regular, and Johnson solids. The table compares the symmetry and congruency properties of the classes. The symbols embedded on the polyhedra show the distinct types of faces/edges/vertices present in them.

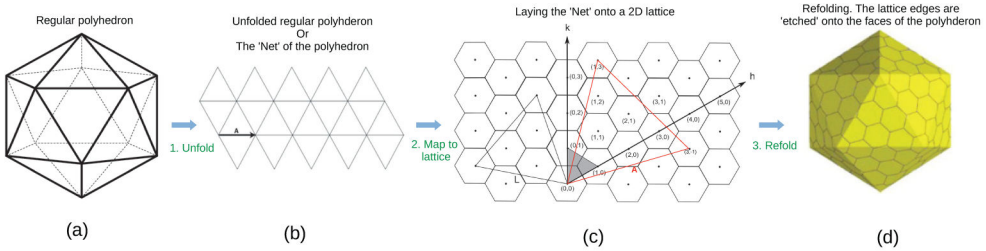

Fig. 5. Illustration of the Goldberg construction

The Goldberg construction involves unfolding an icosahedron (see **(a)** and **(b)**), and then mapping the unfolded icosahedron onto a 2D hexagonal lattice scaled and oriented such that all corners of the unfolded icosahedron (its original vertices) fall on the centers of some hexagon of the grid (some example scale and orientations (for one triangle only) are shown **(c)**). Finally, the icosahedron is folded back, along with the hexagonal grid etched onto its faces. For example, for the scaling and orientation of the red triangle in **(c)**, would result in the tiled icosahedron shown in **(d)**. Notice that the new polyhedron has exactly 12 regular pentagonal faces, where the icosahedral vertices originally were, and many regular hexagonal faces.

TilingGen($\mathcal{P}$, $\mathcal{L}$, h, k)
Constructs an *almost-regular* polyhedron using compatible mapping of polyhedron $\mathcal{P}$ onto lattice $\mathcal{L}$, such that the scaling and combinatorics are specified by h,k.

1. Assume that the lattice coordinate system is aligned with the Cartesian coordinate system such that the origings coincide and one of the axes is aligned to the X axis, and the other lies on the XY plane.
2. Place one point A at the origin $(0, 0)$ of the lattice, a second point at (h, k). Compute the other corners of the face $\mathcal{T}$. Note that we only need to know the number of vertices n of $\mathcal{T}$.
3. Compute the location of the center D of the face $\mathcal{T}$.
4. Let $\mathbb{T}_{\mathbb{C}}$ be the set of cyclic symmetry operations around D, such that $|\mathbb{T}_{\mathbb{C}}| = n$.
5. Initialize empty set $\mathbb{S}$
6. For each lattice point p inside or on $\mathcal{T}$ do
7. Add p to $\mathbb{S}$ if none of the transformations in $\mathbb{T}_{\mathbb{C}}$ applied to p produces a point which is already in $\mathbb{S}$.
8. Compute the transformation T_{map} which maps the face $\mathcal{T}$ to a face of the polyhedron $\mathcal{P}$. T_{map} is composed of $T_{map_T} T_{map_S} T_{map_A}$ such that T_{map_A} translates $\mathcal{T}$ along the lattice to take D to the origin O, T_{map_S} is a scaling that resizes $\mathcal{T}$ to the size of the faces in $\mathcal{P}$, then T_{map_T} is a translation along Z-axis by an amount equal to the distance from the center of $\mathcal{P}$ to a face-center.
9. Let $\mathbb{T}_{\mathbb{P}}$ be the set of global symmetry operations (from the symmetry group of $\mathcal{P}$).
10. Define a set of transformations $\mathbb{T}_{all} = \{T_2 T_{map} T_1 | T_2 \in \mathbb{T}_{\mathbb{P}} \& T_1 \in \mathbb{T}_{\mathbb{S}}\}$.
11. All points on the almost-regular polyhedron is now generated by simply computing $\mathbb{T}_{all}(\mathbb{S})$.

Fig. 6.

TilingGen: Algorithm for constructing an *almost-regular* polyhedron using compatible mapping

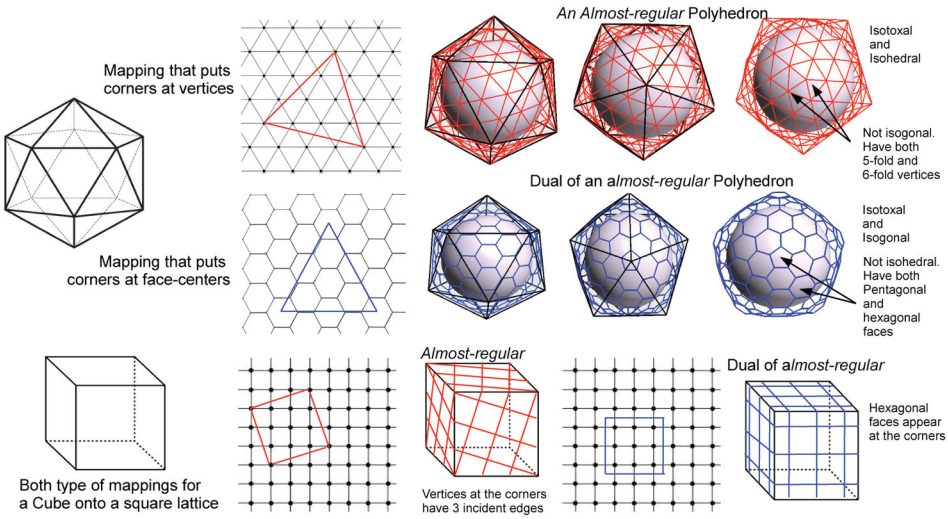

Fig. 7. Illustration of the constructing *almost-regular* polyhedron and their duals

Top row shows how placing corners of a polyhedral face on vertices of a compatible lattice produces an *almost-regular* polyhedron. The black lines show the original polyhedron, and the red lines show the etching/tiling induced by the lattice. The second row shows and example of placing the corners at face centers and producing duals of *almost-regular* polyhedron. Finally, the bottom row shows examples of both the primal and the dual constructions using a square lattice.

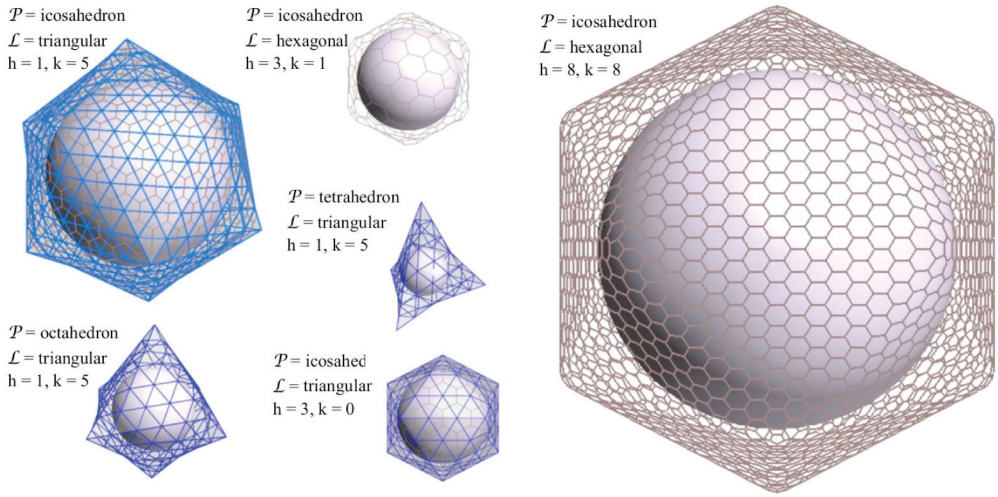

Fig. 8. Some polyhedron generated by applying TilingGen.

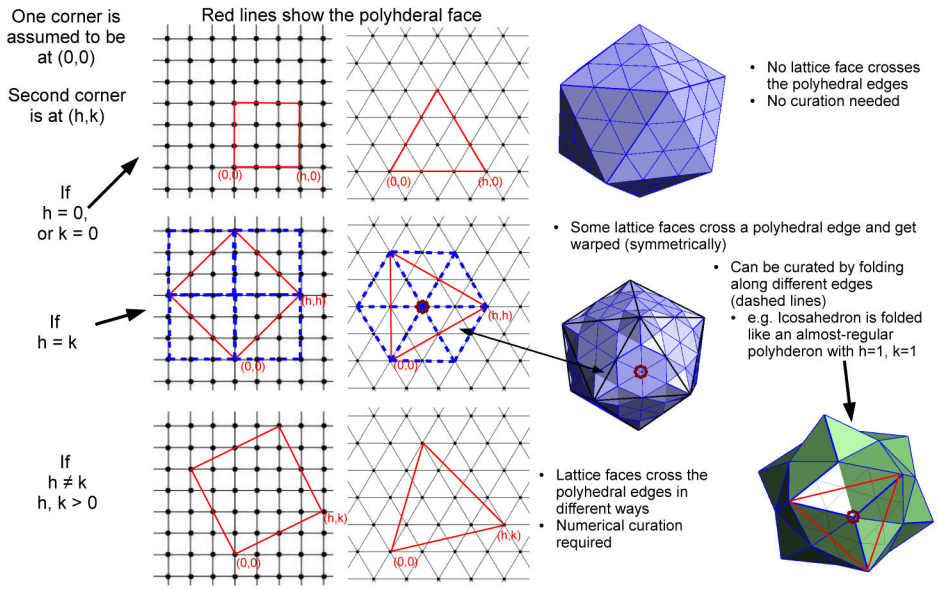

Fig. 9.
Different cases of warping of tiles, and their curations.

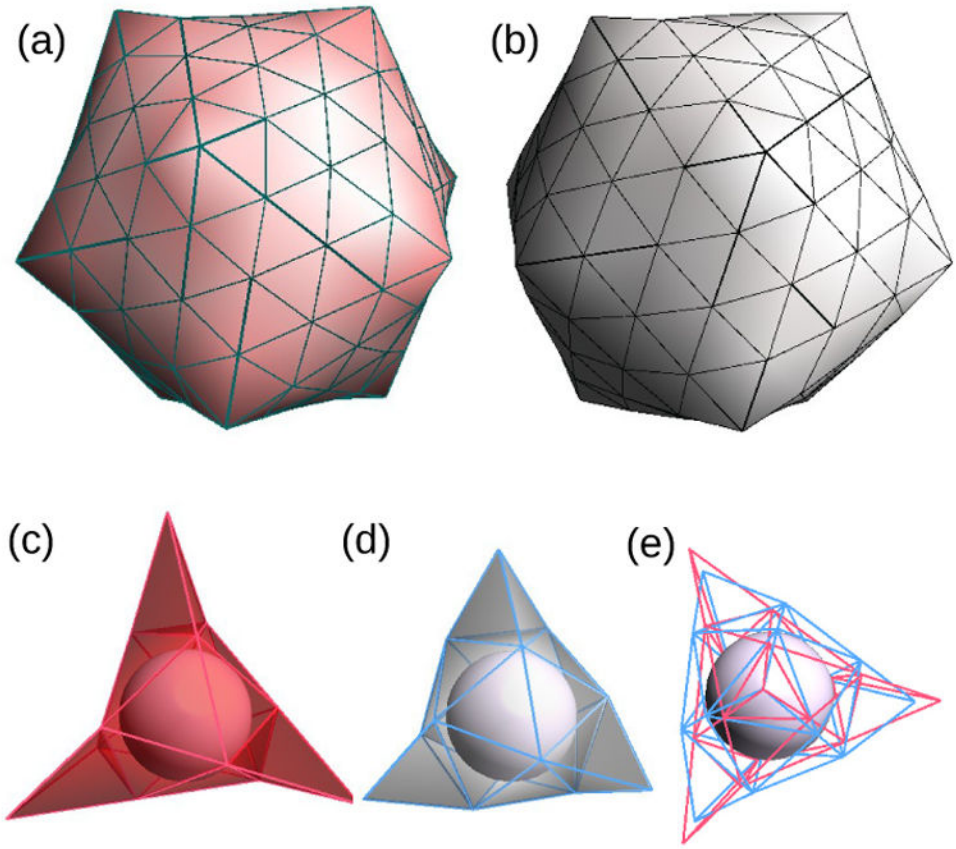

Fig. 10. Numerical curation of warped faces

Top row: (a) shows a polyhedron with icosahedral symmetry and 260 tiles. The color of the triangles are determined by the ratio of the longest and the shortest edge of the tile. Ratios 1 to 1.3+ are colored using white to red gradient. The triangles at the corners and near the edges of the icosahedron have higher distortion. (b) shows the result of numerical curation. All the triangles are now regular, the worst ratio being 1.034, and the symmetry is preserved. Bottom row: (c–d) show a similar before-after figure for a smaller polyhedra, but one where the warping is more apparent. The numerical optimization brought down the ratio of the worst triangle from 2.13 to 1.004. (e) shows a superposition of the two states to highlight that points are updated symmetrically.

ShellGen(n, B) Given integer n and the structure (and relevant parameters) of building block B, construct a shell with icosahedral symmetry.

1. Find integer solutions for h and k such that $c(h^2 + hk + k^2) = n$, where c is the local symmetry order of the face of the tiling (3 for icosahedral).
2. If no integer solutions are found
3. Terminate.
4. Else
5. Construct a meshed polyhedra or a tiling τ with icosahedral symmetry and the solved values of h, k.
6. Construct a cyclic symmetric super-block SB using c copies of B.
7. Symmetrically (see Appendix for detail) place a copy of SB on each tile of τ.
8. Search over the space of in-plane rotations and radial translations (symmetrically applied to each SB).
9. Report the highest scoring model.

Fig. 11.

ShellGen: Algorithm for constructing a shell structure template upon an *almost-regular* of requisite size.

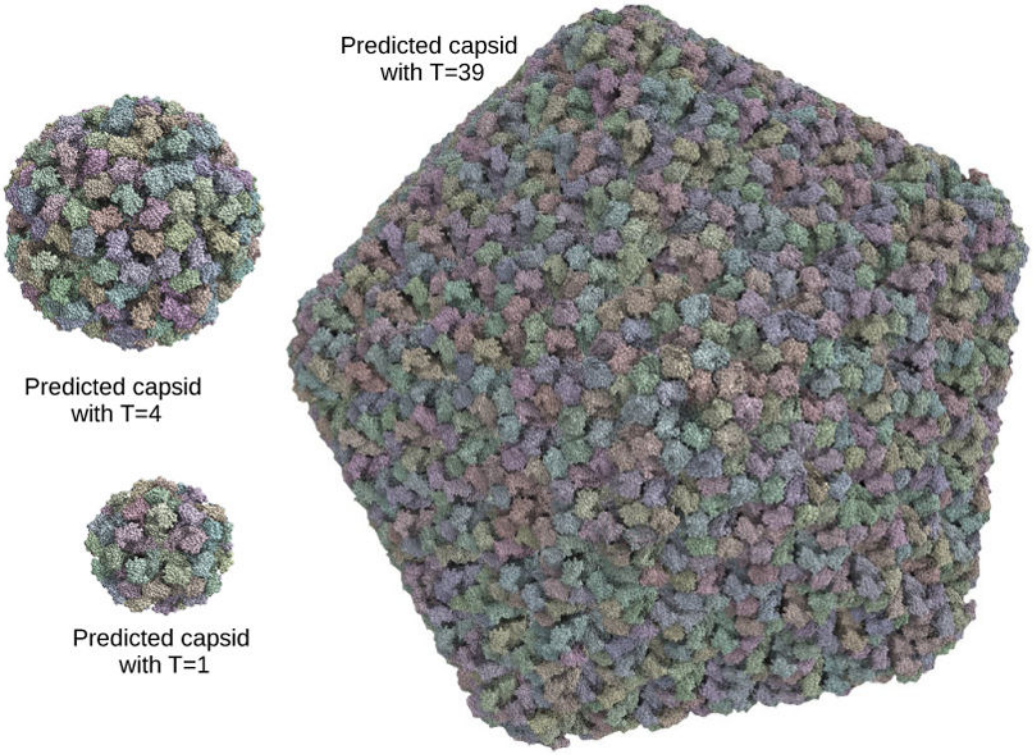

Fig. 12.
Shells of different sizes using the same protein

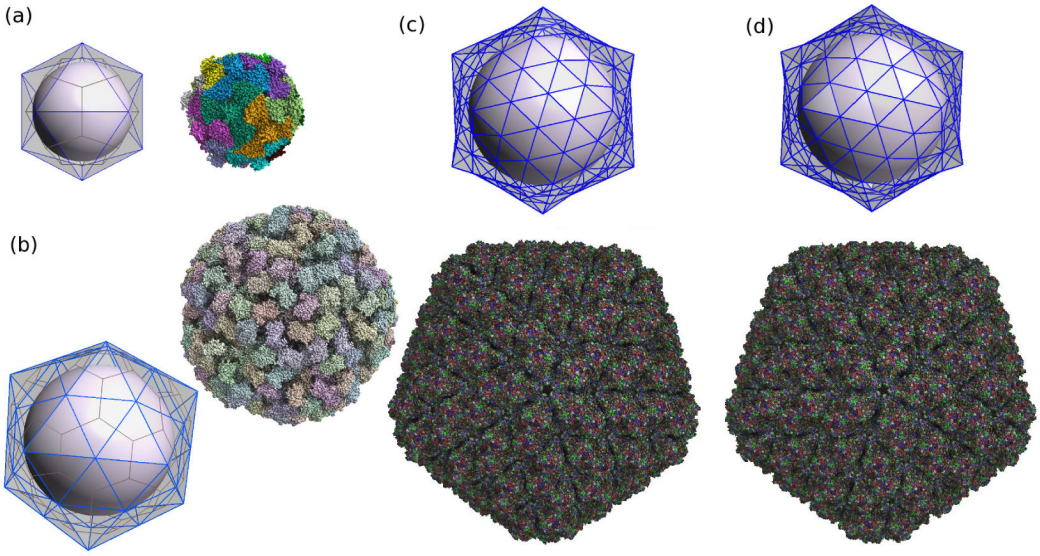

Fig. 13. Predicted shell structures for known viruses

(a) Predicted shell structure for Tobacco Necrosis Virus using a polyhedra with h=1, k=0. (b) Predicted shell structure for Nudaurelia Capensis Virus using a polyhedron with h=2, k=0. (c) Predicted shell structure for Rice Dwarf Virus outer shell using h=1, k=3. (d) Predicted structure for the same virus with h=3, k=1. All the predicted models have the correct inter-tile (or inter-protein) interfaces/contact in terms of geometry, and have the correct global and local topology; except, the one in (c) which has wrong chilarity).